

Heterogeneous Mean First Passage Time Scaling in Fractal Media

Hyun-Myung Chun,¹ Sungmin Hwang,² Byungnam Kahng,³ Heiko Rieger,^{4,5} and Jae Dong Noh⁶

¹*School of Physics, Korea Institute for Advanced Study, Seoul 02455, Korea*

²*Capital Fund Management, 75007 Paris, France*

³*Center for Complex Systems Studies, and KENTECH Institute for Grid Modernization, Korea Institute of Energy Technology, Naju 58217, Korea*

⁴*Center for Biophysics and Department of Theoretical Physics, Saarland University, 66123 Saarbrücken, Germany*

⁵*Lebniz-Institute for New Materials INM, 66123 Saarbrücken, Germany*

⁶*Department of Physics, University of Seoul, Seoul 02504, Korea*

(Dated: May 1, 2023)

The mean first passage time (MFPT) of random walks is a key quantity characterizing dynamic processes on disordered media. In a random fractal embedded in the Euclidean space, the MFPT is known to obey the power law scaling with the distance between a source and a target site with a universal exponent. We find that the scaling law for the MFPT is not determined solely by the distance between a source and a target but also by their locations. The role of a site in the first passage processes is quantified by the random walk centrality. It turns out that the site of highest random walk centrality, dubbed as a hub, intervenes in first passage processes. We show that the MFPT from a departure site to a target site is determined by a competition between direct paths and indirect paths detouring via the hub. Consequently, the MFPT displays a crossover scaling between a short distance regime, where direct paths are dominant, and a long distance regime, where indirect paths are dominant. The two regimes are characterized by power laws with different scaling exponents. The crossover scaling behavior is confirmed by extensive numerical calculations of the MFPTs on the critical percolation cluster in two dimensional square lattices.

Random walks are fundamental for stochastic processes, such as transport, search, and spreading. While random walks on regular lattices have long been studied [1], there has been an ever-increasing interest in the topic incorporating structural disorder of the underlying substrate [2], geometric confinement [3], stochastic resetting [4], non-Markovian dynamics [5], and many more.

An important quantity characterizing random walks (RWs) is the first passage time (FPT) distribution and the mean first passage time (MFPT) [1, 6]. Scaling properties of the FPT and MFPT reflect the interplay between the RW-dynamics and geometric properties of the underlying substrate. For example, on infinite lattices, the FPT distribution follows a power law with a universal exponent [1, 6]. Generally, in finite scale-invariant media, the MFPT $T(r)$ between two sites at a distance r is known to obey the scaling law [7–9]

$$T(r) \sim \begin{cases} Nr^{d_w - d_f}, & \text{for } d_w > d_f, \\ N \ln r, & \text{for } d_w = d_f, \\ N, & \text{for } d_w < d_f. \end{cases} \quad (1)$$

where N is the total number of sites, d_f is the fractal dimension of the medium, and d_w is its walk dimension. It is remarkable that the scaling law is governed by only one universal exponent, $\theta = d_w - d_f$. On the other hand, on a highly heterogeneous graph, the MFPT displays a more complex scaling behavior [10–12]. In a scale-free network characterized by a power-law distribution of local connectivity of each site, the FPT and the MFPT averaged over source sites display a target site dependent scaling behavior [12]. Generally, in heterogeneous

media, the MFPT from site i to j could be very different from the MFPT from j to i : for undirected graphs, one can assign a potential-like quantity, called the RW centrality (RWC), to each site [13]. Since the MFPT between two sites in either direction differs by the difference in their inverse RWCs (see below), a wide distribution of the RWCs could lead to a source-target specific, or heterogeneous, scaling of the MFPT, which is what we will address in this paper.

To this purpose, we reconsider the scaling law in Eq. (1) for two-dimensional (2D) critical bond percolation clusters. We will show that despite a homogeneous local connectivity distribution, the MFPT displays a heterogeneous scaling behavior characterized by a site-dependent scaling exponent and an intriguing crossover scaling, for which the site with the highest RWC is responsible. RWs on critical percolation clusters have long been studied [2, 14–17], but a site-dependent or heterogeneous scaling has not been reported yet. Our work also sheds light on the role of the RWC for RWs in disordered media.

We consider an undirected graph consisting of N sites, whose connectivity is represented with a symmetric adjacency matrix $A = A^T$ whose matrix elements A_{ij} are 0 or 1 indicating the absence or presence of an edge between sites i and j [18], respectively. The number of edges attached to a site i is its degree and is given by $k_i = \sum_j A_{ij}$. A discrete time RW on the graph is defined by the transition matrix $W = K^{-1}A$, where K is a diagonal matrix with $K_{ij} = \delta_{ij}k_i$. That is, a random walker at site i jumps to site j with the probability $W_{ij} = A_{ij}/k_i$

in a unit time step $\Delta t = 1$. The transition matrix has the left row eigenvector $\langle \pi | = (\pi_1, \dots, \pi_i, \dots, \pi_N)$ with $\pi_i = k_i / (\sum_j k_j)$ and the right column eigenvector $|\mathbf{1}\rangle = (1, 1, \dots, 1)^T$, both with eigenvalue $\lambda = 1$. The left eigenvector corresponds to the steady state probability distribution [13].

A general theoretical framework for studying discrete time random walks has been formulated some time ago [1, 13, 19]. There the MFPT from site i to j is given by [13]

$$T_{ij} = \frac{R_{jj} - R_{ij} + \delta_{ij}}{\pi_j}, \quad (2)$$

where the matrix R is called the group generalized inverse of $(I - W)$ in mathematical literature [20, 21] and given by $R \equiv \sum_{t=0}^{\infty} (W^t - |\mathbf{1}\rangle\langle \pi|)$ [22]. In Eq. (2), the diagonal element $T_{ii} = 1/\pi_i = (\sum_j k_j)/k_i$ has the meaning of the *mean first return time*. Condamin *et al.* [7] noticed that R_{ij} is dominated by the term $\sum_{t=0}^{\infty} W(j, t|i)$ where $W(j, t|i) \equiv (W^t)_{ij}$ is the probability to find the walker at site j in t steps when it started at site i . Assuming the scaling form $W(j, t|i) = t^{-d_f/d_w} \Pi\left(\frac{r_{ij}}{t^{1/d_w}}\right)$ with r_{ij} being the Euclidean distance between i and j [2], they derived the scaling law in Eq. (1) [7].

The formal expression in Eq. (2) has a deeper implication when the transition probabilities satisfy the detailed balance condition, $\pi_i W_{ij} = \pi_j W_{ji}$ for all i and j , which holds for RWs on undirected graphs. Then, one can assign an RWC $C_i = \pi_i / R_{ii}$ to each site i , relating the MFPTs T_{ij} and T_{ji} by [13]

$$T_{ij} - T_{ji} = C_j^{-1} - C_i^{-1}. \quad (3)$$

The RWC is an indicator of the attractiveness of a site in the random walk process: a first passage to a higher RWC site from a lower RWC site takes less time than the first passage in the opposite direction. The RWC has also been used to identify influential nodes in complex networks [23–27]. The inverse of the RWC $\alpha_i \equiv 1/C_i = R_{ii}/\pi_i$ is equal to the average MFPT to site i from a random departure site j sampled with the steady state probability distribution, $\alpha_i = \sum_{j \neq i} \pi_j T_{ji}$. It is also called the global mean first passage time [10, 28], or the accessibility index [29]. Similarly, Kemeny's constant is defined as $K_i = \sum_{j \neq i} T_{ij} \pi_j = \sum_j R_{jj}$ [19, 29]. Interestingly, it is independent of i and serves as a characteristic of the global structure of an underlying graph [30].

In a disordered medium site-to-site fluctuations of the RWC may affect the scaling of the MFPT with the distance. We address this issue for the RW on the critical bond percolation cluster of 2D square lattices [2, 3, 14–16], which we generate by occupying bonds of a 2D $L \times L$ square lattice with periodic boundary conditions with the critical occupation probability $p_c = 1/2$ and identifying the largest cluster. The 2D critical percolation cluster is a random fractal with the fractal dimension $d_f = 91/48$ [31]. The walk dimension is known to be $d_w \simeq 2.87 > d_f$ [32].

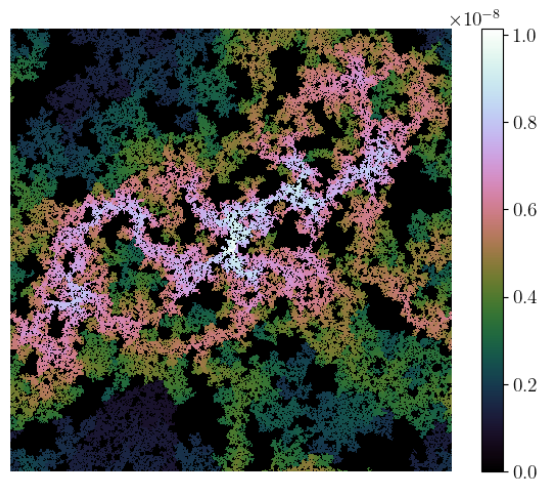


FIG. 1. RWC configuration on a 2D critical percolating cluster in a lattice of size 1024×1024 . The hub is located at the center of the lattice. The black area represents sites that do not belong to the percolating cluster.

It is computationally demanding to evaluate the RWC and the MFPT for it requires to find the group generalized inverse of $I - W$ [25]. We will adapt the numerical algorithm developed in Ref. [33], which turns out to be extremely efficient. It takes only a few minutes in an ordinary desktop computer to compute the RWC distribution for the critical percolation cluster of lattices of size 1024×1024 . It also allows one to evaluate the MFPTs from a few selected sites to all the other sites at a similar computing cost. All numerical data reported in the paper are obtained on lattices of size 1024×1024 , if not stated otherwise, and averaged over at least 2000 independent realizations of the critical percolation cluster.

Figure 1 illustrates an RWC configuration on a critical bond percolation cluster. The RWC distribution is highly heterogeneous (see App. A). High RWC sites are clustered and spread out in a filamentous pattern, which is analogous to the backbone structure [2]. This heterogeneity raises questions about the simple scaling of the MFPT with a single scaling exponent as in Eq. (1).

To highlight the site dependence of the MFPT, we identify the *hub* (highest RWC site) and the *marginal site* (lowest RWC site), and measure the average outbound/inbound MFPTs to/from all the other sites at a given distance r . As shown in Fig. 2, the outbound MFPT is larger than the inbound MFPT for the hub, and vice versa for the marginal site. The difference is exactly given by the difference in the inverse RWCs (see Eq. (3)). The MFPTs scale algebraically with L and r as

$$T \sim L^\Delta r^\theta \quad (4)$$

with the scaling exponents Δ and θ . Surprisingly, the hub and the marginal site are characterized by different

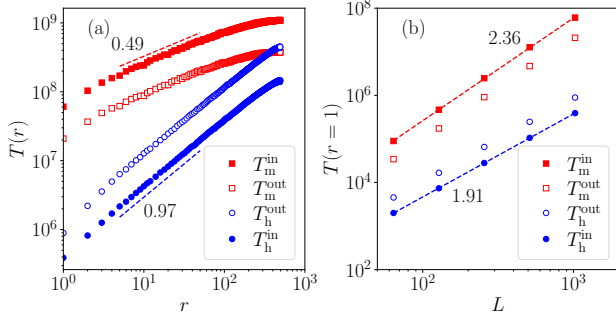


FIG. 2. (a) Average MFPT between the hub (circular symbols) or the marginal site (rectangular symbols) with the other sites. The outbound and inbound MFPTs are marked with empty and filled symbols, respectively. In (b), we plot the MFPTs from/to sites at a unit distance $r = 1$ as a function of the linear system size $64 \leq L \leq 1024$. The scaling exponents are obtained by fitting the data within the range indicated by the dashed lines.

scaling exponents

$$\theta = \begin{cases} \theta_h \simeq 0.97(5), & \text{for the hub} \\ \theta_m \simeq 0.49(5), & \text{for the marginal site.} \end{cases} \quad (5)$$

The exponent θ_h associated with the hub is close to the exponent $d_w - d_f = 0.97(4)$ of Eq. (1) in value. On the other hand, the MFPT at the marginal site grows with a considerably smaller exponent $\theta_m \simeq 0.49$ (see App. B for detailed analysis). The finite size scaling exponent Δ also varies. It takes on $\Delta_h \simeq 1.90$ for the hub, which is in agreement with the fractal dimension $d_f = 91/48$ of Eq. (1) [7]. The marginal site displays a stronger finite size effect with $\Delta_m \simeq 2.36 > \Delta_h$.

We note that $\Delta_h + \theta_h \simeq \Delta_m + \theta_m$. It is understood from the site independence of Kemeny's constant [29]. Kemeny's constant evaluated at a site i is given by $K_i = \sum_{j \neq i} T_{ij} \pi_j$. Since $\pi_j = a_j/N$ with $O(1)$ constant a_j , Kemeny's constant is approximated as the arithmetic average of outbound MFPTs to all the other sites. The scaling form in Eq. (4) leads to $K \sim L^{\Delta+\theta}$. Thus, $\Delta + \theta$ should be the same at the sites obeying Eq. (4). We also note that the inbound and outbound MFPTs differ by a constant factor. The difference $|T^{\text{in}}(r) - T^{\text{out}}(r)|$ is equal to the difference in the accessibility index of a source and target site at a distance r . Thus, we infer that the MFPT and the accessibility index difference follow the same scaling law. From now on, we focus our study on the outbound MFPT.

The site-dependent scaling behavior is not limited to an exceptional outlier site: We consider the outbound MFPTs from a set of source sites $\{M_1, M_2, \dots\}$ selected hierarchically as follows. We select the local minimum RWC site M_n among all sites within a circle of radius $R_n = 2^{n-1}$ centered at the hub. The outbound MFPT $T_n(r)$ from M_n was measured as a function of the distance

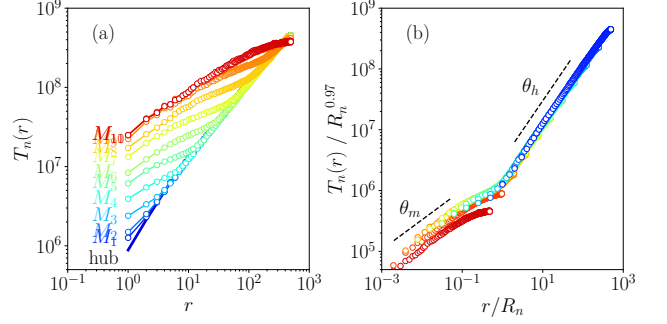


FIG. 3. (a) Outbound MFPT T_n from the site M_n (thin lines with symbols). Also shown is the MFPT from the hub (thick line). (b) Scaling plot of $T_n(r)/R_n^{\theta_h}$ vs r/R_n with $R_n = 2^{n-1}$. The dashed lines of slope θ_h and θ_m given in Eq. (5) are guides to the eye.

r to target sites. The result is shown in Fig. 3(a). We find an interesting crossover of $T_n(r)$. It grows algebraically with r with the exponent θ_m for $r \ll R_n$ and with the exponent θ_h for $r \gg R_n$. The crossover scaling behavior is summarized by the scaling form

$$T_n(r) = N R_n^{\theta_h} \mathcal{F}(r/R_n), \quad (6)$$

where the scaling function $\mathcal{F}(x)$ has the limiting behaviors $\mathcal{F}(x \ll 1) \sim x^{\theta_m}$ and $\mathcal{F}(x \gg 1) \sim x^{\theta_h}$. The crossover scaling is confirmed by the scaling plot shown in Fig. 3(b).

The observed crossover is also a generic phenomenon. We investigated the outbound MFPT from a set of sites $\{A_1, A_2, \dots\}$ where A_n is an arbitrary site selected randomly among the sites at a distance $R_n = 2^{n-1}$ from the hub. We found that the MFPT $T'_n(r)$ from A_n also exhibits the crossover scaling of the form (6). In Fig. 4(a), we plot the ratio of $T'_n(r)$ to $T_h(r)$ to highlight the crossover. It clearly shows that $T'_n(r)/T_h(r)$ deviates from 1 for $r \ll R_n$ and converges to 1 for $r \gg R_n$. Interestingly, the scaling exponent in the regime $r \ll R_n$ is given by $\theta_a \simeq 0.84(5) \neq \theta_m$. It is close to θ_h , but not the same.

The exponent θ_a also governs the scaling of MFPT from a randomly selected source site A (see Fig. 4(b)). In Fig. 4(b), we compare the average value $T_A(r)$ and the standard deviation $\delta T_A(r)$ of the MFPTs from A to sites at a distance r . The fluctuation is even larger than the mean value for $r \ll L$. This strong non-self-averaging behavior is another indication of the heterogeneity.

Our numerical results highlight the role of the maximum RWC site in the random walk dynamics. Imagine an ensemble of the first passage events from a source site s to a target site t at a distance r_{s-t} . Let r_{s-h} be the distance from s to the hub. When the target is farther than the hub ($r_{s-t} \gg r_{s-h}$), the ensemble is dominated by the paths detouring via the hub. Consequently the MFPT follows the scaling $T \sim r^{\theta_h}$ with the scaling expo-

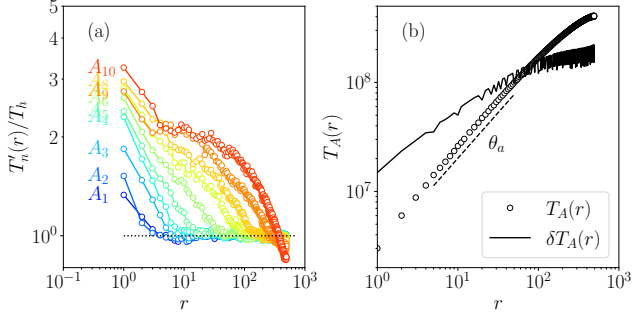


FIG. 4. (a) MFPT $T'_n(r)$ from a site A_n at a distance $R_n = 2^{n-1}$ from the hub normalized by $T_h(r)$. The horizontal dotted line is a guide to the eye. (b) MFPT $T_A(r)$ from an arbitrary source site selected randomly. It follows a power law scaling $T_A(r) \sim r^{\theta_a}$ with $\theta_a \simeq 0.84$.

nent $\theta_h = d_w - d_f$ irrespective of s . On the other hand, when the target is closer than the hub ($r_{s-t} \ll r_{h-s}$), the ensemble is dominated by direct paths and the MFPT scaling law depends on the choice of s . The crossover may be overlooked when one measures the MFPT averaged over all pairs of source and target sites at a given distance.

One can understand the origin (and potential complications) of the scaling law for $T(r)$ in Eq. (1) [7] by the following consideration: Given a source-target pair at a distance r , one partitions the entire graph into blocks of linear size $\xi_r \sim r$, putting the source and target into the same block denoted as starting block. Each block has $N_r \sim r^{d_f}$ sites and the total number of blocks is $\mathcal{N}_r \sim N/N_r \sim N r^{-d_f}$. If all blocks were statistically equivalent, the RW would always spend $\tau_r \sim r^{d_w}$ time steps in a single block until it hops to a neighboring block. With Eq. (2) the return time to the starting block is $T_{\text{ret.}} \sim \tau_r \cdot (1/\pi_b)$, with the probability to be in one block $\pi_b \sim 1/\mathcal{N}_r \sim r^{d_f}/N$, thus $T_{\text{ret.}} \sim N r^{d_w - d_f}$. The MFPT can then be estimated as $T_{\text{ret.}}/P_s$, with P_s the probability to find the target site before leaving the starting block, which is $P_s = O(1)$ for $d_w > d_f$ and $P_s \sim \tau_r/N_r \sim r^{d_w - d_f}$ for $d_w < d_f$. This argument reproduces the scaling law Eq. (1), except for the marginal case $d_w = d_f$. It clearly reveals that the simple scaling, $T(r) \sim r^\theta$ with a unique scaling exponent θ , is based on the assumption that the entire fractal lattice can be partitioned into homogeneous blocks. Our results presented in Figs. 3 and 4, however, indicate that blocks are heterogeneous on all length scales.

This heterogeneity is further evidenced by the scaling behavior of the chemical distance (number of edges in the shortest path) $l(r)$ with respect to the Euclidean distance between two sites. The average chemical distance is known to scale as $l(r) \sim r^{d_{\text{min.}}}$, with $d_{\text{min.}} \simeq 1.14$ for the 2D critical percolation cluster (Sec. 6.6 of [34]). We discriminate again between the hub (h) and the marginal

site (m) as starting site and found

$$l(r) \sim \begin{cases} L^{\delta_h} r^{d_{\text{min.},h}}, & \delta_h \simeq 0.0, \quad d_{\text{min.},h} \simeq 1.11 \\ L^{\delta_m} r^{d_{\text{min.},m}}, & \delta_m \simeq 0.52, \quad d_{\text{min.},m} \simeq 0.58 \end{cases} \quad (7)$$

The chemical distance $l_n(r)$ from the local minimum RWC site M_n shows again a crossover $l_n(r) = L^{\delta_h} R_n^{d_{\text{min.},h}} \mathcal{G}(l/R_n)$ for $1 \ll R_n \ll L$. We also looked at the MFPT as a function of the chemical distance and observed a similar crossover behavior (see App. C for the detailed analysis for the chemical distance scaling).

To conclude, we report in this paper, for the first time, heterogeneous scaling behavior of the MFPT of RWs on a random fractal, the critical percolation cluster in 2D (similarly in 3D [35], see App. D). MFPTs measured from the hub and measured from the marginal site as a function of the distance of the target site obey power law scaling with distinctively different exponents and the distance dependence of MFPTs from general starting sites shows a striking crossover. Heterogeneous behavior of various observables in disordered systems is expected, as for instance dynamical heterogeneities in glassy systems [36] or in the context of Griffiths singularities in strongly disordered systems [37] like the transverse Ising chain [38] or the Sinai walk [39]. A lack of self-averaging is a prominent consequence of this spatial heterogeneity [40], and it manifests itself in the quantities we looked at. But different power laws for different regions in the system, as we find them for regions close to the hub and close to the marginal site, have, to our knowledge, not been reported before. An important consequence of our results is that scaling theories for the MFPT that are based on an explicit or hidden spatial homogeneity assumption should be considered more carefully. The critical percolation cluster consists of a backbone, dangling ends, and red bonds [2, 41]. We suspect that low RWC sites may belong to dangling ends with high probability being separated from the bulk sites with red bonds. One possibility is that the scaling law (1) might be restricted to the backbone. The scaling exponents associated with the marginal site might have some scaling relations with the fractal dimension of the dangling ends and red bonds. We have to postpone checking these possibilities to future work. Finally, for the quantity we looked at, the MFPT, the origin of this strong heterogeneity can be traced back to the broad distribution of the RWC in critical percolation clusters, which indicates that our results could be generalized to, and are relevant for, a larger class of complex networks.

J.D.N was supported by the National Research Foundation of Korea (NRF) grant funded by the Korea government (MSIP) (Grants No. 2019R1A2C1009628). HR acknowledges financial support by the German Research Foundation (DFG) within the Collaborative Research Center SFB 1027. H.-M.C. was supported by a KIAS Individual Grant (PG089401) at Korea Institute for Advanced Study.

-
- [1] B. D. Hughes, *Random walks and random environments. Volume 1: Random walks* (Clarendon Press, 1995).
- [2] S. Havlin and D. Ben-Avraham, Diffusion in disordered media, *Advances in Physics* **51**, 187 (2002).
- [3] O. Bénichou, C. Chevalier, J. Klafter, B. Meyer, and R. Voituriez, Geometry-controlled kinetics, *Nature Chemistry* **2**, 472 (2010).
- [4] M. R. Evans, S. N. Majumdar, and G. Schehr, Stochastic resetting and applications, *Journal of Physics A* **53**, 193001 (2020).
- [5] A. Barbier-Chebbah, O. Bénichou, and R. Voituriez, Self-Interacting Random Walks: Aging, Exploration, and First-Passage Times, *Physical Review X* **12**, 011052 (2022).
- [6] S. Redner, *A Guide to First-Passage Processes* (Cambridge University Press, New York, 2001).
- [7] S. Condamin, O. Bénichou, V. Tejedor, R. Voituriez, and J. Klafter, First-passage times in complex scale-invariant media, *Nature* **450**, 77 (2007).
- [8] S. Reuveni, R. Granek, and J. Klafter, Vibrational shortcut to the mean-first-passage-time problem, *Physical Review E* **81**, 040103 (2010).
- [9] A. Roberts and C. Haynes, Electrostatic approximation of source-to-target mean first-passage times on networks, *Physical Review E* **83**, 031113 (2011).
- [10] V. Tejedor, O. Bénichou, and R. Voituriez, Global mean first-passage times of random walks on complex networks, *Physical Review E* **80**, 065104(R) (2009).
- [11] V. Tejedor, O. Bénichou, and R. Voituriez, Close or connected: Distance and connectivity effects on transport in networks, *Physical Review E* **83**, 066102 (2011).
- [12] S. Hwang, D. S. Lee, and B. Kahng, First Passage Time for Random Walks in Heterogeneous Networks, *Physical Review Letters* **109**, 088701 (2012).
- [13] J. D. Noh and H. Rieger, Random Walks on Complex Networks, *Physical Review Letters* **92**, 118701 (2004).
- [14] J. C. A. d'Auriac, A. Benoit, and R. Rammal, Random walk on fractals: numerical studies in two dimensions, *Journal of Physics A* **16**, 4039 (1983).
- [15] S. Alexander and R. Orbach, Density of states on fractals : « fractons », *Journal de Physique Lettres* **43**, 625 (1982).
- [16] O. Bénichou, B. Meyer, V. Tejedor, and R. Voituriez, Zero constant formula for first-passage observables in bounded domains, *Physical review letters* **101**, 130601 (2008).
- [17] S. Condamin, V. Tejedor, R. Voituriez, O. Bénichou, and J. Klafter, Probing microscopic origins of confined subdiffusion by first-passage observables, *Proceedings of the National Academy of Sciences* **105**, 5675 (2008).
- [18] The formalism in the paper is also valid in a weighted graph with non-binary adjacency matrix elements.
- [19] J. G. Kemeny and J. L. Snell, *Finite Markov Chains* (Springer, New York, 1976).
- [20] C. D. Meyer, Jr, The Role of the Group Generalized Inverse in the Theory of Finite Markov Chains, *SIAM Review* **17**, 443 (1975).
- [21] J. J. Hunter, The Role of Kemeny's Constant in Properties of Markov Chains, *Communications in Statistics - Theory and Methods* **43**, 1309 (2014).
- [22] The matrix $(I - W)$ is not invertible because one of the eigenvalues of W equals to 1. The group generalized inverse is defined as $\sum_{n=2}^N \frac{1}{1-\lambda_n} |\lambda_n\rangle\langle\lambda_n|$, where λ_n , $|\lambda_n\rangle$, $\langle\lambda_n|$ are the n -th eigenvalue, right eigenvector, and left eigenvector of W , respectively. The sum excludes the eigenstate with $\lambda_1 = 1$.
- [23] M. Loecher and J. Kadtke, Enhanced predictability of hierarchical propagation in complex networks, *Physics Letters A* **366**, 535 (2007).
- [24] F. Blöchl, F. J. Theis, F. Vega-Redondo, and E. O. Fisher, Vertex centralities in input-output networks reveal the structure of modern economies, *Physical Review E* **83**, 046127 (2011).
- [25] B. C. Johnson and S. Kirkland, Estimating random walk centrality in networks, *Computational Statistics & Data Analysis* **138**, 190 (2019).
- [26] S. Oldham, B. Fulcher, L. Parkes, A. Arnatkevičiūtė, C. Suo, and A. Fornito, Consistency and differences between centrality measures across distinct classes of networks, *PloS one* **14**, e0220061 (2019).
- [27] A. P. Riascos, D. Boyer, P. Herringer, and J. L. Mateos, Random walks on networks with stochastic resetting, *Physical Review E* **101**, 062147 (2020).
- [28] Z. Zhang, Y. Qi, S. Zhou, S. Gao, and J. Guan, Explicit determination of mean first-passage time for random walks on deterministic uniform recursive trees, *Physical Review E* **81**, 016114 (2010).
- [29] S. Kirkland, Random walk centrality and a partition of Kemeny's constant, *Czechoslovak Mathematical Journal* **66**, 757 (2016).
- [30] S. Yilmaz, E. Dudkina, M. Bin, E. Crisostomi, P. Ferraro, R. Murray-Smith, T. Parisini, L. Stone, and R. Shorten, Kemeny-based testing for covid-19, *Plos one* **15**, e0242401 (2020).
- [31] D. Stauffer and A. Aharony, *Introduction to percolation theory*, 2nd ed. (Taylor & Francis, London, 1992).
- [32] I. Majid, D. Avraham, S. Havlin, and H. Stanley, Exact-enumeration approach to random walks on percolation clusters in two dimensions, *Physical Review B* **30**, 1626 (1984).
- [33] S. Hwang, D.-S. Lee, and B. Kahng, Fast algorithm for relaxation processes in big-data systems, *Physical Review E* **90**, 043303 (2014).
- [34] D. Ben-Avraham and S. Havlin, *Diffusion and reactions in fractals and disordered systems* (Cambridge university press, 2000).
- [35] C. D. Lorenz and R. M. Ziff, Precise determination of the bond percolation thresholds and finite-size scaling corrections for the sc, fcc, and bcc lattices, *Physical Review E* **57**, 230 (1998).
- [36] W. Kob, C. Donati, S. J. Plimpton, P. H. Poole, and S. C. Glotzer, Dynamical Heterogeneities in a Supercooled Lennard-Jones Liquid, *Physical Review Letters* **79**, 2827 (1997); W. K. Kegel and Blaaderen, and Alfons van, Direct Observation of Dynamical Heterogeneities in Colloidal Hard-Sphere Suspensions, *Science* **287**, 290 (2000).
- [37] F. Iglói and C. Monthus, Strong disorder RG approach of random systems, *Physics Reports* **412**, 277 (2005).
- [38] D. S. Fisher, Random transverse field Ising spin chains, *Physical Review Letters* **69**, 534 (1992); Critical behavior of random transverse-field Ising spin chains, *Physical Review B* **51**, 6411 (1995); F. Iglói and H. Rieger, Random transverse Ising spin chain and random walks,

- Physical Review B **57**, 11404 (1998).
- [39] D. S. Fisher, P. L. Doussal, and C. Monthus, Random Walks, Reaction-Diffusion, and Nonequilibrium Dynamics of Spin Chains in One-Dimensional Random Environments, Physical Review Letters **80**, 3539 (1998); F. Iglói and H. Rieger, Anomalous diffusion in disordered media and random quantum spin chains, Physical Review E **58**, 4238 (1998).
 - [40] A. Aharony and A. B. Harris, Absence of Self-Averaging and Universal Fluctuations in Random Systems near Critical Points, Physical Review Letters **77**, 3700 (1996-10); S. Wiseman and E. Domany, Finite-Size Scaling and Lack of Self-Averaging in Critical Disordered Systems, Physical Review Letters **81**, 22 (1998).
 - [41] H. J. Herrmann, D. C. Hong, and H. E. Stanley, Backbone and elastic backbone of percolation clusters obtained by the new method of 'burning', Journal of Physics A **17**, L261 (1999).

Supplemental Materials

Hyun-Myung Chun¹, Sungmin Hwang², Byungnam Kahng³, Heiko Rieger^{4,5}, and Jae Dong Noh⁶

¹*School of Physics, Korea Institute for Advanced Study, Seoul 02455, Korea*

²*Capital Fund Management, 75007 Paris, France*

³*Center for Complex Systems Studies, and KENTECH Institute for Grid Modernization, Korea Institute of Energy Technology, Naju 58217, Korea*

⁴*Center for Biophysics and Department of Theoretical Physics, Saarland University, 66123 Saarbrücken, Germany*

⁵*Lebniz-Institute for New Materials INM, 66123 Saarbrücken, Germany*

⁶*Department of Physics, University of Seoul, Seoul 02504, Korea*

Appendix A: Distribution of the Random Walk Centrality

We investigate statistical properties of the random walk centrality or the accessibility index of sites in the 2D critical percolation cluster. Given a percolation cluster, we measure the accessibility indices α of all sites and construct a histogram of them normalized by the average value $\langle\alpha\rangle$. The probability distribution function $P(\alpha/\langle\alpha\rangle)$ is then obtained by taking the average of the histogram over the ensemble of percolation clusters. In Fig. S1(a), we present and compare the distribution functions at three different values of L . They overlap one another, which indicates that the accessibility distribution is characterized with only a single scale, namely the mean value $\langle\alpha\rangle$. The distribution function has asymmetric Gaussian tails.

We also study the system size dependence of the mean value $\langle\alpha\rangle$, the minimum value α_H of the hub, and the maximum value α_M of the marginal site. Their ensemble averaged values follow the power law $\alpha \sim L^{2.88(1)}$ with the same exponent close to the random walk ex-

ponent d_w . The accessibility index α_i has a meaning of the average MFPT to i from all the other sites. It is surprising that the average MFPT to the most accessible site (hub) and the least accessible site (marginal site) follow the finite-size scaling law with the same exponent. This indicates that the average quantity alone is not a useful measure. The structural heterogeneity is not captured by the finite size scaling behavior of the average MFPT.

Figure S1(c) presents the distribution functions of the maximum accessibility index $\alpha_M/\langle\alpha\rangle$ and the maximum random walk centrality $\langle\alpha\rangle/\alpha_H$, normalized with $\langle\alpha\rangle$. The distribution functions are comparable with the Gumbel distribution which governs the extreme value statistics of Gaussian-distributed random variables.

Appendix B: Distance Dependent MFPT

We have shown in the main text the MFPTs from the hub and the marginal site follow a power law scaling

$$T(r) \sim L^\Delta r^\theta \quad (\text{S1})$$

with distinct scaling exponents $(\Delta_h, \theta_h) \simeq (1.90, 0.97)$ for the hub and $(\Delta_m, \theta_m) \simeq (2.36, 0.49)$ for the marginal site. We also measure $T_A(r)$, the average MFPT from an arbitrary source site selected *at random*. As shown in Fig. S2(a), $T_A(r)$ also follows the scaling law of Eq. (S1). The scaling exponent is obtained from an effective exponent analysis. The MFPTs within the range $r/\sqrt{2} < r_0 < \sqrt{2}r$ are fitted to yield the effective exponent $\theta(r)$. Figure S2(c) presents the effective exponents for θ_h for the hub, θ_m for the marginal site, and θ_a for a random site. The asymptotic scaling exponent is given by the limiting value in the $r \rightarrow \infty$ and $L \rightarrow \infty$ limit. The effective exponents for θ_h and θ_m converge to the values obtained from the global fitting in the main text. The effective exponent for θ_a converges to $\theta_a = 0.84(5)$. The three distinct scaling exponents θ_h , θ_m , and θ_a signify the strong structural heterogeneity in the first passage processes.

The strong heterogeneity weakens when one adopts the chemical distance instead of the Euclidean distance as seen in Fig. S2(b) and (d). The chemical distance depen-

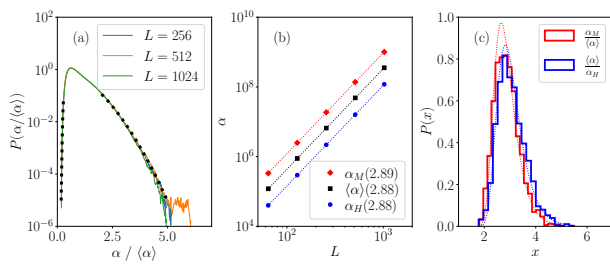


FIG. S1. (a) Distribution functions of the normalized accessibility index. The tails are fitted well by Gaussian functions (dashed lines) with different stiffness on either side. (b) System size dependence of the accessibility indices of the hub (α_H), the marginal site (α_M), and the mean value ($\langle\alpha\rangle$). The figure in the legend refers to the finite-size scaling exponent. (c) Distribution functions (solid lines) of the largest accessibility index and the largest random walk centrality (inverse accessibility index). They are compared with the Gumbel distribution function (dotted lines) $P_G(x) = \exp\left[(x - \mu)/\beta - e^{-(x - \mu)/\beta}\right]/\beta$ with μ and β being determined from the mean and the variance of the data.

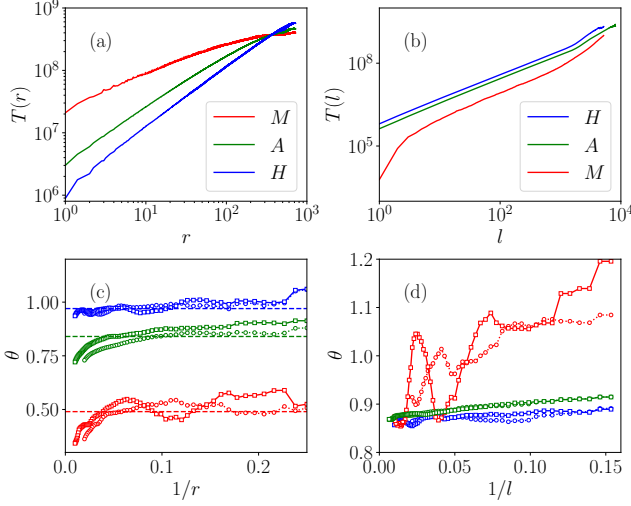


FIG. S2. (a) Euclidean distance (r) dependence and (b) chemical distance (l) dependence of the MFPTs from the hub (H), the marginal site (M), and an arbitrary site selected at random (A) at $L = 1024$. (c) The effective exponents for the power law scaling $T(r) \sim r^\theta$ at $L = 512$ (circular symbols) and $L = 1024$ (square symbols). The asymptotic values are marked with the dashed lines. (d) The effective exponents for the power law scaling $T(l) \sim l^{\theta_l}$ at $L = 512$ (circular symbols) and $L = 1024$ (square symbols).

dent scaling behavior will be discussed in the proceeding App. C.

Appendix C: MFPT vs Chemical Distance

Structural heterogeneity of the critical percolation cluster is evidenced by the scaling behavior of the chemical distance $l(r)$ with respect to the Euclidean distance between two sites. The chemical distance between two sites is defined as the number of edges in the shortest path connecting them. It is known that the *average* chemical distance $l(r)$ between any pairs of sites at a distance r scales as $l(r) \sim r^{d_{\min.}}$ with the chemical distance exponent $d_{\min.}$ (Sec. 6.6 of [34]), which is for 2D critical percolation clusters $d_{\min.} \simeq 1.14$. We discriminate between the hub and the marginal site as starting site and find

$$l(r) \sim L^\delta r^{d_{\min.}} \quad (\text{S1})$$

with *different* exponents $(\delta, d_{\min.}) = (\delta_h, d_{\min.,h}) \simeq (0.0, 1.11)$ for the hub and $(\delta_m, d_{\min.,m}) \simeq (0.52, 0.58)$ for the marginal site (see Figs. S3(a) and (b)), satisfying $\delta_h + d_{\min.,h} \simeq \delta_m + d_{\min.,m}$. The chemical distance $l_n(r)$ from the local minimum RWC site M_n shows again a crossover $l_n(r) = L^{\delta_h} R_n^{d_{\min.,h}} \mathcal{G}(l/R_n)$ for $1 \ll R_n \ll L$ (see Figs. S3(c) and (d)).

Given the similar crossover scaling of $T_n(r)$ and $l_n(r)$, one may anticipate a simple scaling, $T(l) \sim l^{\theta_l}$ with a

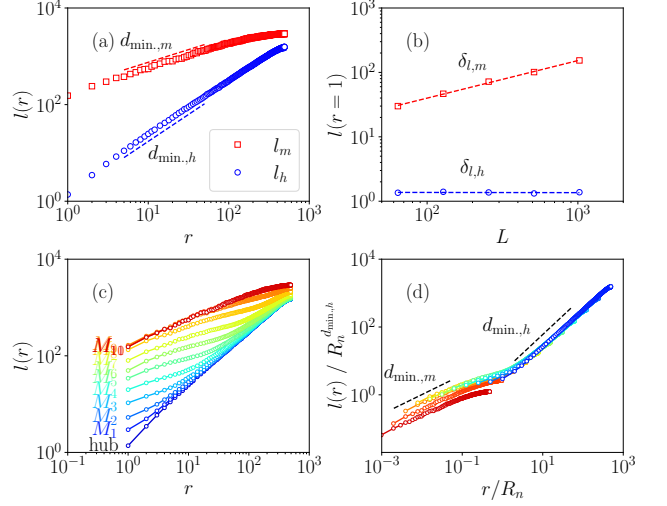


FIG. S3. (a) Chemical distance $l_{h/m}(r)$ from the hub/marginal site. (b) System size L dependence of $l_{h/m}(r=1)$. These plots confirm the power law scaling of Eq. (7) with $\delta_h = 0$, $\delta_m \simeq 0.52$, $d_{\min.,h} \simeq 1.11$, and $d_{\min.,m} \simeq 0.58$. (c) Chemical distance $l_n(r)$ from the local minimum RWC site M_n . (d) Scaling plot of $l_n(r)/R_n^{d_{\min.,h}}$ against r/R_n . $L = 1024$ in (a), (c), and (d).

unique exponent $\theta_l = \theta/d_{\min.}$, of the MFPT with respect to the chemical distance. Such a simple scaling behavior of the average MFPT was indeed reported in Ref. [16, 17]. We have investigated the source site dependence of the MFPT function $T_n(l)$. Figure S4(a) shows the $T_h(l)$ from the hub follows the power law scaling

$$T_h(l) \sim l^{\theta_l} \quad (\text{S2})$$

with $\theta_l \simeq 0.88$. This exponent satisfies the scaling relation $\theta_l = \theta_h/d_{\min.,h}$. The MFPT $T_n(l)$ from the local minimum RWC sites still displays a crossover, albeit weak. The crossover is more evident in Fig. S4(b). $T_n(l)$ undergoes a crossover between two limiting behaviors, $T_h(l)$ of the hub and $T_m(l)$ of the marginal site, at a characteristic scale of the chemical distance $l_n \sim R_n^{d_{\min.}}$ (see Fig. S4(c)). The numerical data suggest that

$$T_m(l) = T_h(l)/(a - b/\ln(cl)) \quad (\text{S3})$$

with $O(1)$ constants a , b , and c (see Fig. S4(b)). The logarithmic correction results in the slow convergence of the effective exponent θ_a in Fig. S2(d).

Appendix D: Crossover in 3D Critical Percolation Cluster

The crossover scaling is not limited to the 2D critical percolation clusters. We have investigated the scaling law for the MFPT $T(r)$ on the 3D critical bond percolation clusters. It is known that the critical threshold is given

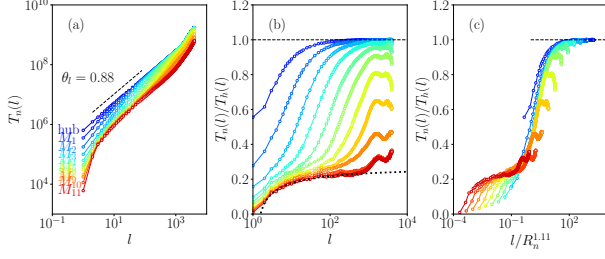


FIG. S4. (a) MFPT vs chemical distance from the hub and the local minimum RWC sites. (b) Ratio of $T_n(l)$ to $T_h(l)$ for $n \geq 1$. For the marginal site, $T_m(l)/T_h(l)$ can be fitted to a function $0.27 - 0.26/\ln(1.70l)$, which is drawn with a dotted line. (c) Scaling plot of $T_n(l)/T_h(l)$ against $l/R_n^{d_{\min}}$.

by $p_c \simeq 0.248\,812\,6$ and the fractal dimension is given by $d_f \simeq 2.523$ [35].

On a critical percolation cluster, we identified the hub H (maximum RWC site), M_n (local minimum RWC site within a sphere of radius $R_n = 2^{n-1}$ around the hub), and the marginal site M (global minimum RWC site). The MFPTs from those sites to the other sites were measured as a function of the distance r . The ensemble aver-

aged MFPTs from the hub and the marginal site satisfy the scaling law $T(r) \sim L^\Delta r^\theta$ with $(\Delta_h, \theta_h) \simeq (2.51, 1.21)$ for the hub and $(\Delta_m, \theta_m) \simeq (2.91, 0.79)$ for the marginal sites (see Figs. S5(a) and (b)). The sums $\Delta_h + \theta_h$ and $\Delta_m + \theta_m$ are close to each other, and consistent with the random walk dimension $d_w \simeq 3.64 \pm 0.05$ [2]. Figure S5(c) shows that the MFPTs $T_n(r)$ from the local minimum RWC sites display the crossover scaling behavior.

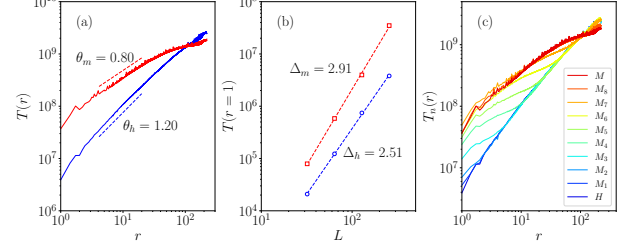


FIG. S5. MFPT on the critical bond percolation cluster in 3D. (a) MFPT $T(r)$ from the hub and the marginal site when $L = 256$. (b) Size dependence of the MFPTs from the hub and the marginal site to the sites at a distance $r = 1$. (c) MFPTs from the hub, the marginal site, and the local minimum RWC sites when $L = 256$.